J Geod (2011) 85:791–805
DOI 10.1007/s00190-011-0464-0

ORIGINAL ARTICLE

GOCE gravitational gradients along the orbit

Johannes Bouman · Sophie Fiorot · Martin Fuchs · Thomas Gruber · Ernst Schrama · Christian Tscherning · Martin Veicherts · Pieter Visser

Received: 5 October 2010 / Accepted: 17 March 2011

Abstract GOCE is ESA's gravity field mission and the first satellite ever that measures gravitational gradients in space, that is, the second spatial derivatives of the Earth's gravitational potential. The goal is to determine the Earth's mean gravitational field with unprecedented accuracy at spatial resolutions down to 100 km. GOCE carries a gravity gradiometer that allows deriving the gravitational gradients with very high precision to achieve this goal. There are two types of GOCE Level 2 gravitational gradients (GGs) along the orbit: the gravitational gradients in the gradiometer reference frame (GRF) and the gravitational gradients in the local north oriented frame (LNOF) derived from the GGs in the GRF by point-wise rotation. Because the V_{XX}, V_{YY}, V_{ZZ} and V_{XZ} are much more accurate than V_{XY} and V_{YZ}, and because the error of the accurate GGs increases for low frequencies, the rotation requires that part of the measured GG signal is replaced by model signal. However, the actual quality of the gradients in GRF and LNOF needs to be assessed. We analysed the outliers in the GGs, validated the GGs in the GRF using independent gravity field information and compared their assessed error with the requirements. In addition, we compared the GGs in the LNOF with state-of-the-art global gravity field models and determined the model contribution to the rotated GGs. We found that the percentage of detected outliers is below 0.1% for all GGs, and external gravity data confirm that the GG scale factors do not differ from one down to the 10^{-3} level. Furthermore, we found that the error of V_{XX} and V_{YY} is approximately at the level of the requirement on the gravitational gradient trace, whereas the V_{ZZ} error is a factor of 2–3 above the requirement for higher frequencies. We show that the model contribution in the rotated GGs is 2–35% dependent on the gravitational gradient. Finally, we found that GOCE gravitational gradients and gradients derived from EIGEN-5C and EGM2008 are consistent over the oceans, but that over the continents the consistency may be less, especially in areas with poor terrestrial gravity data. All in all, our analyses show that the quality of the GOCE gravitational gradients is good and that with this type of data valuable new gravity field information is obtained.

Keywords GOCE · Gravitational gradients · External calibration · Tensor rotation

J. Bouman (✉) · M. Fuchs
Deutsches Geodätisches Forschungsinstitut (DGFI), Munich, Germany
e-mail: bouman@dgfi.badw.de

S. Fiorot
SRON Netherlands Institute for Space Research, Utrecht, The Netherlands

T. Gruber
Institut für Astronomische und Physikalische Geodäsie (IAPG), TU München, Munich, Germany

E. Schrama · P. Visser
Delft Institute of Earth Observation and Space Systems (DEOS), TU Delft, Delft, The Netherlands

C. Tscherning · M. Veicherts
Niels Bohr Institute, University of Copenhagen, Copenhagen, Denmark

1 Introduction

Since October 2009 GOCE delivers gravitational gradients (GGs) along the orbit. These Level 2 gravitational gradients in the instrument frame are used in combination with the GOCE GPS tracking data to model the Earth's gravitational field (Pail et al. 2011). In addition, the gravitational gradients themselves may be used in Earth science

applications with or without rotation to, for example, a local north oriented frame, e.g. (Pedersen and Rasmussen 1990; Mikhailov et al. 2007). The goal of this paper is to show how the GOCE Level 2 gravitational gradients are computed and to assess their quality and information content. As input the Level 1b gravitational gradients are being used (Frommknecht et al. 2011).

We will first summarize in Sect. 2 the preprocessing of the gravitational gradients in the gradiometer reference frame (GRF), which is the instrument frame fixed to the satellite. The method is discussed in detail in (Bouman et al. 2009) and is briefly summarized here. We will focus on the results with real data and discuss their performance. Second, we will address the rotation of the gravitational tensor from the GRF to the local north-oriented frame (LNOF). The GOCE gravitational gradients V_{XX}, V_{YY}, V_{ZZ} and V_{XZ} are more accurately measured than V_{XY} and V_{YZ}, where the accurate gravitational gradients have the smallest error in the measurement band (MB) between 5 mHz and 0.1 Hz. A rotation from the GRF to any other frame will in principle project part of the larger V_{XY} and V_{YZ} error onto the other gravitational gradients in the rotated frame, see (Müller 2003). In addition, the 1/f GG error for longer wavelengths may leak into the MB after tensor rotation (Bouman 2007). The method to circumvent these problems is described in Sect. 3. In brief, the GOCE V_{XY} and V_{YZ} GGs as well as the signal of all GGs below the MB are replaced with gravitational gradients from a GOCE gravity field model. We will address how to combine the GOCE GGs and model GGs. Furthermore, we will study how much of the original observed GOCE GGs is contained in the rotated GGs as compared with the model GGs. The GGs in the LNOF are assessed and compared with GRACE-based gravity field information.

2 Gravitational gradient preprocessing

2.1 Preprocessing at the high-level processing facility

The main goal of the GOCE mission is to provide a model of the Earth's mean gravity field (ESA 1999), and therefore the GOCE gravitational gradients need to be corrected for temporal gravity field variations. Also outliers that may occur in the GOCE gravitational gradients need to be searched for and detected in the preprocessing step (Bouman 2004). Along with the external calibration of the gravitational gradients (Bouman et al. 2004), their error needs to be assessed (Bouman and Koop 2003). The steps for GG preprocessing therefore are

1. Correction for temporal gravity field variations;
2. Outlier detection and flagging;
3. External calibration and error assessment.

These preprocessing steps lead to corrected and calibrated Level 2 GGs in the GRF, which are one of the GOCE final products (EGG_NOM_2). These GGs are input to the gravity field analysis as well as to the frame transformation, which leads to GGs in the LNOF (EGG_TRF_2). The frame transformation, or tensor rotation, is discussed in Sect. 3, whereas the GOCE gravity field analyses are covered in (Pail et al. 2011). See also (Bouman et al. 2007; Förste et al. 2007; Migliaccio et al. 2004; Pail and Plank 2004). The different steps of the GG preprocessing method are summarized in Sect. 2.2, for a detailed description, see (Bouman et al. 2009).

2.2 Gravitational gradients in the gradiometer reference frame

2.2.1 Corrections for temporal gravity field variations

We discern tidal and non-tidal temporal gravity field variations. For the tidal GG correction, we consider a number of tidal effects acting on the gradiometer, which are all second-order derivatives of the astronomical tide-generating potential: the indirect solid Earth tide deformation potential, the self attraction and loading deformation potential and the pole tide potential. For the non-tidal GG correction we take into account the most prominent high-frequency signals from atmospheric and oceanic mass variations as well as seasonal variations derived from a GRACE gravity field time series. For the latter, it is assumed that it contains information about seasonal time variable gravity signal from all other sources (continental water, ice mass variations and solid Earth mass variations). In our processing chain, a set of gravity potential correction coefficients is computed for every 6 h, which further is used to compute gravitational gradient corrections for all six tensor elements. For a more complete description of the temporal gravity field variations and how they are computed see (Bouman et al. 2009).

The gravitational gradient temporal gravity field signals are in general very small at GOCE altitude compared with the GG signal and error. As an example, Fig. 1 displays the gravitational gradient trace and the gravitational gradient temporal V_{ZZ} corrections for 1 November 2009. The gravitational gradient trace is not zero due to the errors in the diagonal gravitational gradients. Thus, the temporal gravitational gradient signals are about two orders smaller or more than these errors at all frequencies.

2.2.2 Outlier detection

The GGs data screening method adopted for the diagonal GGs V_{XX}, V_{YY} and V_{ZZ} is based on three tests:

1. The trace of the gradient tensor is zero (Laplace condition);

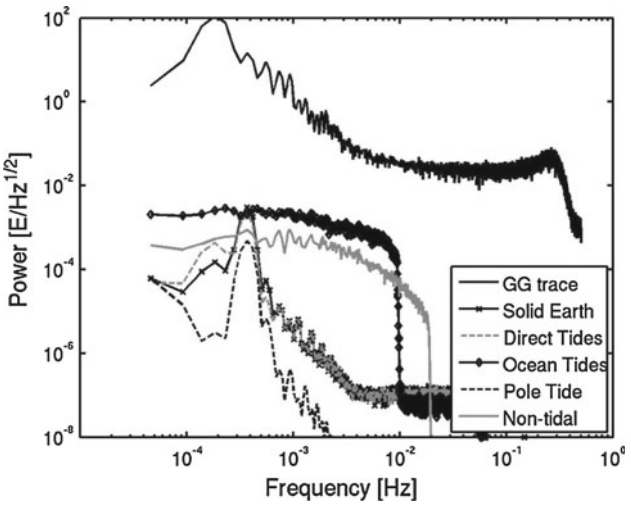

Fig. 1 Spectral density of 1 day (1 November 2009) of the GG trace and V_{ZZ} temporal signals in EGG_NOM_2

2. the difference between the observed GGs and gradients from a selected global model is zero (test on GG anomalies); and
3. the difference between cubic spline interpolated and observed GG anomalies from (2) is zero (spline test).

If the trace test indicates a data point as an outlier and this is confirmed by one or both of the other two tests, it is flagged as such (Bouman 2004). For the off-diagonal components V_{XY}, V_Z and V_{YZ}, the trace test is not applicable. Therefore, to flag an off-diagonal component as an outlier, both tests on the GG anomalies must indicate an outlier to flag the data point as such. Flagged data points are discarded in the external calibration and error assessment. Should the number of flagged data points be larger than a certain threshold, e.g. 1% of daily arcs, then the automated process is put on hold and the data will be examined in more detail. The detected outliers are indicated in the external calibrated GG file (EGG_NOM_2) by a flag. If less than five consecutive epochs are detected as outliers, then the EGG_NOM_2 file will contain a fill-in value, see (Gruber et al. 2007). Details on the outlier detection algorithm as well as the performance of the single tests and their combination can be found in (Bouman 2004; Bouman et al. 2009).

In this section we present statistics on outliers in the GOCE GG data collected in the period 31 October 2009 to 26 June 2010. Only a few outliers were detected, nearly all in the diagonal terms V_{XX}, V_{YY} and V_{ZZ}. The mean number of outliers detected within a week in these GGs is, respectively, 253, 156 and 327, which represents 0.04, 0.03, 0.06% of the weekly data (sampling rate is 1 s, 1 week has 604,800 epochs). The mean number of outliers stays stable in time. In Table 1 we can see that the standard deviations of these means are small. The off-diagonal terms are almost not flagged and the mean of detected outliers is about 6 per week for the V_{XZ} component. Bouman et al. (2009) found that for simulated GOCE data the Type I error is 0.02% for the diagonal gravitational gradients and 0.00% for the off-diagonal gravitational gradients. These numbers are very close to what we find here for real data and therefore a large part of the detected outliers is probably a Type I error, that is, the observation is not an outlier but resides in the tail of the distribution.

As mentioned earlier, the criteria to flag a data point as outlier are different for diagonal and off-diagonal terms. The trace test and the difference test detect, respectively, about 1,800 and 3,000 epochs per week, which is much more than the spline test with a mean of detected outliers around 15. The trace and the difference tests flag different epochs because the number of detected outliers is much less than that indicated by the individual tests. An analysis of the flagged data points shows that data with high and sharp peaks are flagged. In addition, sometimes data are flagged that are not obvious outliers but as the total percentage of flagged data points is small, the percentage of incorrectly flagged data points will be small as well. Slow and smooth oscillations are hard or impossible to detect with our method, even if they have a relatively high amplitude (up to a few E), which can be the case after a data gap triggering a Kalman reinitialisation.

Besides this quantitative analysis, it is interesting to pay attention to the geographical distribution of these outliers. It appeared that no general pattern can be observed. The outliers are randomly located over the orbits, as illustrated by Fig. 2.

Table 1 Percentage of detected outliers, based on weekly data

GG	Mean	Standard deviation	Minimum	Maximum
V_{XX}	4.3×10^{-2}	8×10^{-3}	3.1×10^{-2}	5.8×10^{-2}
V_{YY}	2.6×10^{-2}	5×10^{-3}	1.8×10^{-2}	3.6×10^{-2}
V_{ZZ}	5.5×10^{-2}	6×10^{-3}	4.7×10^{-2}	7.3×10^{-2}
V_{XY}	1.2×10^{-4}	4×10^{-4}	0	2.1×10^{-3}
V_{XZ}	9.6×10^{-4}	1×10^{-3}	0	7.1×10^{-3}
V_{YZ}	2.4×10^{-4}	8×10^{-4}	0	4.1×10^{-3}

Period between 31 October 2009 and 26 June 2010

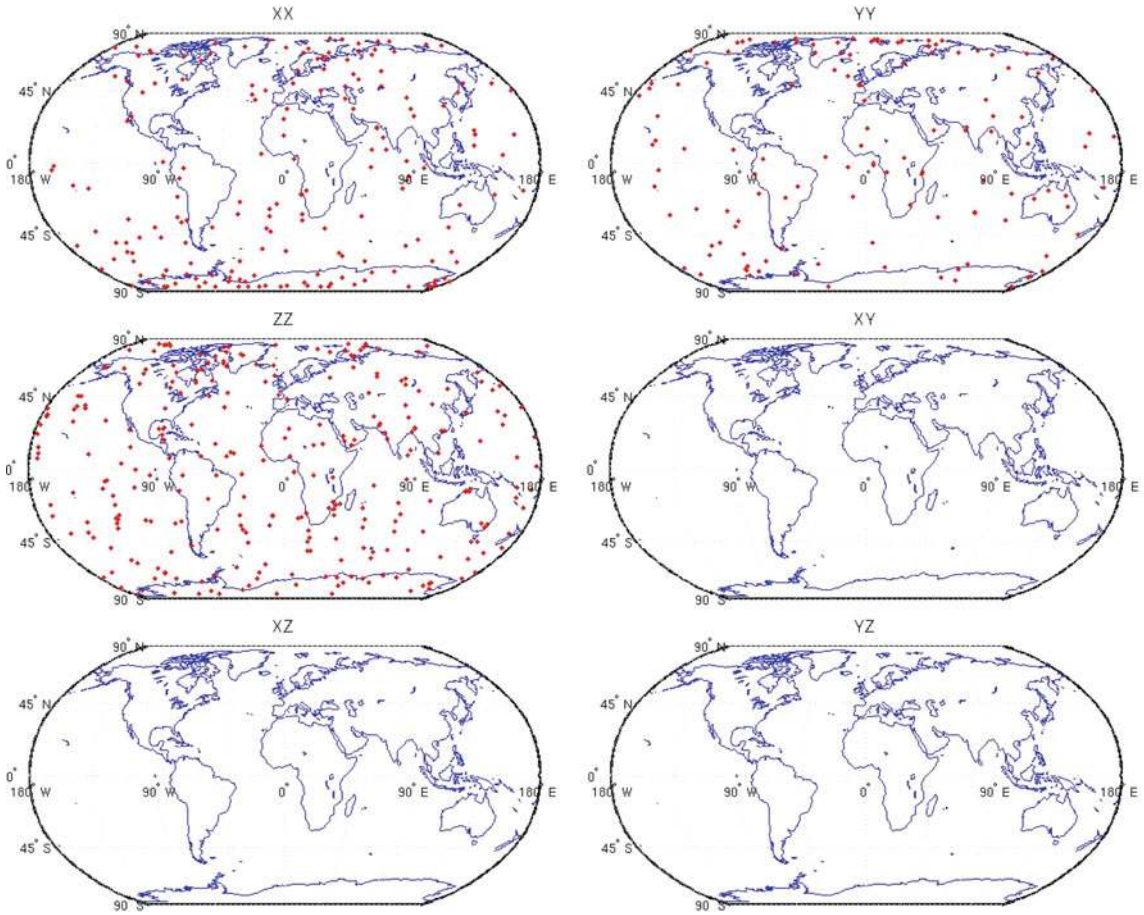

Fig. 2 Geographical of the detected outliers—Period 14 March 2010 to 20 March 2010

2.2.3 External calibration using a global gravity field model

Three different methods are used in the external calibration of the GOCE GGs. The baseline method is the calibration using a global gravity field model, which is used to compute model GGs at satellite level and these GGs serve as reference values for the GOCE GGs to determine, for example, GG scale factors (discussed in this section). A second calibration method uses GOCE SST data and GOCE GGs to estimate the spherical harmonics of a global gravity field model, truncated at degree and order 80, together with calibration parameters (see Sect. 2.2.4). The third calibration method uses terrestrial gravity data. Least-squares collocation (LSC) is used to compute GGs at satellite altitude from the gravity data in selected regions. These GGs serve as reference values with which the GOCE GGs may be calibrated (see Sect. 2.2.5).

The external calibration using a global gravity field model determines scale factors between the measured gravitational gradients, internally calibrated, corrected for temporal effects and outliers flagged and the modeled gravitational gradients calculated with the EIGEN-5C model. Because of the 1/f behaviour of the measured gravitational gradients error, these GGs and the modeled GGs are high-pass filtered (Butterworth, second order). Initially, different filter cut-off frequencies were used in the range between 0.1 and 1 mHz. However, based upon our experience with the science data of GOCE, we now consider higher cut-off frequencies, which are 2, 3, 5 and 7 mHz. The scale factors calculated with the latter present the best consistency across weeks. Hence, four series of scale factors (for each cut-off frequency, a series of six scale factors, and one per GG component) are calculated for each period. The one that minimizes the standard deviation of the trace in the MB is considered to be optimal. It is these values that we present here from the beginning of the science mode period 31 October 2009 of GOCE up to 26 June 2010. In the default process the scale factors are calculated based upon 1 week of data. They also can be calculated with less data if a complete week is not available, but such results are not presented here.

Figure 3 shows the optimal scale factors versus time. There is one plot for each of the six gravitational gradient components. The time, from 31 October 2009 to 26 June 2010, is indicated in GPS seconds. Some scale factors are missing

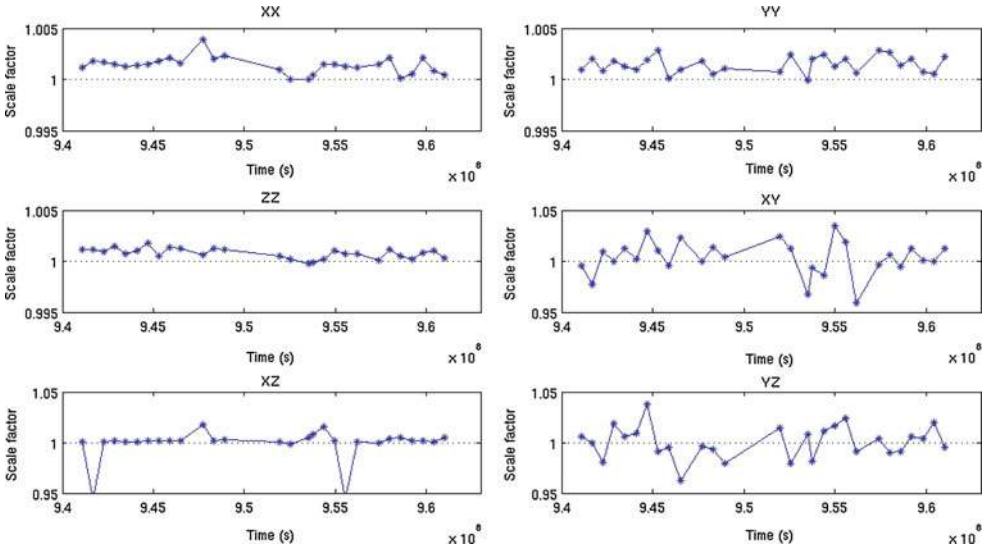

Fig. 3 History of the optimal scale factors calculated by the external calibration using a global gravity field. Period 31 October 2009 to 26 June 2010

because they could not be calculated because of missing data. In January and May 2010, two shakings of the satellite were done by ESA to determine new internal calibration parameters and therefore no data were available for these days and no weekly scale factors could be determined. Some daily ones were calculated but are not included in this plot. In February 2010, GOCE did not provide any data because of a telemetry problem. The plots confirm the good consistency of the optimal scale factors across the weeks.

The scale factor consistency is also due to the fact that the GGs are high-pass filtered and not affected much by slow oscillations such as Kalman reinitialisation oscillations triggered by a data gap, which occurred twice in the studied time window: in November 2009 and April 2010. It appears that only the V_{XZ} GG scale factors are affected. When analysing the GG data it is not obvious why V_{XZ} is affected and the diagonal GGs not, but it may be caused by the smaller signal power in V_{XZ} as compared with the diagonal GGs, which may make V_{XZ} more susceptible to Kalman reinitialisations. The two erroneous V_{XZ} scale factors have similar size because the GG scale factors are not allowed to exceed certain lower and upper bounds that were set based on requirements to the gradiometer.

The optimal scale factors for the four accurate GGs (V_{XX}, V_{YY}, V_{ZZ} and V_{XZ}) provide results very close to one, Table 2. The mean value of the optimal scale factors for each of the diagonal components is 1.0014, 1.0015 and 1.0007, respectively. Moreover the standard deviation is small, between 5×10^{-4} and 8×10^{-4}. For the V_{XZ} component, the mean value is also close to 1 if we drop the two extreme values of November 2009 and April 2010: then, the mean value becomes 1.0031 and the standard deviation 4.3×10^{-3}. Thus, the external calibration confirms the scale factors of the accurate GGs to 10^{-3} as they are provided after L1b processing (Frommknecht et al. 2011). The V_{XY} and V_{YZ} axes are the less accurate gravitational gradients. The optimal scale factors still have a mean value around one but the standard deviation is relatively large, in the order of 1.5×10^{-2}.

2.2.4 Validation of gradiometer observations by GPS

The combination of Satellite-to-Satellite Tracking (SST) observations acquired by the GOCE on-board Global Positioning System (GPS) receiver and Satellite Gravity Gradient (SGG) observations allows the estimation of several

Table 2 Gravitational gradient scale factors: 31 October 2009 to 26 June 2010

Component	Mean	Standard deviation	Minimum	Maximum
V_{XX}	1.0014	8×10^{-4}	1.0000	1.0039
V_{YY}	1.0015	8×10^{-4}	0.9999	1.0029
V_{ZZ}	1.0007	5×10^{-4}	0.9998	1.0017
V_{XY}	1.0030	0.0167	0.9592	1.0341
V_{XZ}	0.9988	0.0159	0.9429	1.0175
V_{YZ}	1.0003	0.0159	0.9621	1.0382

calibration parameters together with the Earth's gravity field. The SST and SGG observations are both complementary and supplementary regarding the observation of the Earth's gravity field, where the SST observations predominantly provide information for the long-to-medium spatial scales (40,000 down to 500 km) and the SGG observations for the medium-to-short spatial scales (from >1,600 to <100 km). Thus, a partial overlap in sensitivity can be identified, which allows for the (implicit) validation of the SGG observations when estimating gravity field parameters from the combination of these observation types.

The gradiometer validation by GPS consists of two modules (Visser 2007). The first module is based on a classical orbit determination process, where calibration and gravity field parameters are included in the estimation process. It is assumed that the GPS SST observations are first reduced to a time series of highly accurate Cartesian X, Y and Z coordinates in an Earth-centred, pseudo-inertial reference frame. For GOCE, these time series are obtained from a kinematic orbit determination (Bock et al. 2010). These time series then serve as observables for the first module. Normal equations will then be formed for a combined least-squares estimation of dynamic orbit and accelerometer calibration parameters and gravity field coefficients based on the numerical integration of the variational equations (Visser et al. 2001). For GOCE, use can be made of the common-mode accelerations to represent the remaining non-gravitational accelerations left by the Drag-Free Control (DFC). These common-mode accelerations are the averages of the in-line observations by each pair of accelerometers. These combinations need to be properly scaled and corrected for constant or slowly drifting offsets (referred to as biases). Typically, orbit determinations are done for daily arcs and the associated normal equations are combined afterwards for the estimation of common parameters, e.g. static gravity field coefficients. This leads to a set of estimated parameters that consists of daily initial conditions for the GOCE orbit (position and velocity at start time), a common-mode bias and scale factor for each gradiometer axis and gravity field parameters in the form of spherical harmonic coefficients. In addition, empirical accelerations are estimated to absorb dynamic modelling errors. The second module provides the normal equations for gravity field coefficients and SGG calibration parameters from the three diagonal SGG components along the satellite orbit, where a precise orbit solution is used for the geo-location. The attitude of the satellite is derived from observations collected by the on-board star trackers, enhanced by angular accelerations observed by the gradiometer.

The first module is built around the NASA/GSFC GEODYN software (Pavlis et al. 2006) and the second module is based on in-house developed software (Visser 2007). The implementation for the High-Level Processing facility (Koop et al. 2006) aims at a validation with minimal latency. Therefore, the data period and maximum spherical harmonic degree of estimated gravity parameters are limited. The GOCE orbit has a repeat period of 61 months with 20-day sub-cycles. Therefore, the baseline period for the validation was taken equal to 20 days, which already provides a homogeneous global coverage as a function of longitude. For each 20 days a gravity field model complete to degree and order 80 was estimated. The additionally estimated parameters consisted of orbital initial conditions (6 per day), common-mode bias and scale factor parameters for all three axes of the gradiometer (3 per day), 1-cycle-per-orbital-revolution (CPR) empirical accelerations (4 per day) and one set of scale factors for the diagonal gravitational gradients (V_{XX}, V_{YY}, V_{ZZ}) for the each period of 20 days (Table 3). It has to be noted that by the high-pass filtering, possible biases are eliminated and in fact become unobservable and are thus not estimated.

As stated earlier, the SST observations were first reduced to time series of kinematic position coordinates. Given the latency requirements, use was made of the Rapid Science

Table 3 Validation of gradiometer observations by GPS: force models and estimated parameter set

Force models	
Static gravity	EIGEN-5S complete to degree and order 150 (Förste et al. 2008)
Solid-earth tides	IERS standards (IERS 2008)
Ocean tides	FES2004 (Lyard et al. 2006)
Temporal gravity	HPF atmosphere and oceans (Koop et al. 2006)
3rd bodies	JPL DE403 planetary ephemeris (Standish et al. 1995)
Non-gravitational	GOCE common-mode accelerations from gradiometer
Estimated parameters	
Gravity field	80 × 80 spherical harmonic coefficients
Orbit (daily)	Initial position and velocity (daily)
	Empirical accelerations: 1 set of sine/cosine 1-cpr (cross-track and radial)
Gradiometer (one set)	Common-mode: three biases and scale factors (X, Y, Z)
	Gravitational gradients: three biases and scale factors (V_{XX}, V_{YY}, V_{ZZ})

The gradiometer X, Y and Z axes are predominantly aligned with the orbital flight, cross-track and negative height direction, respectively

Orbit (RSO) solutions, which have a claimed precision of better than 7 cm for each direction (Bock et al. 2010). The weighting of the associated normal equations is consistent with this precision level. The SGG observations and associated observation equations were high-pass filtered using an inverse *sinc* filter with a stabilizing Hann window (Harris 1978). The resulting normal equations are thus consistent with the applied filtering scheme. The lower frequency cut-off was taken equal to 0.4 mHz or 2 CPR, which leads to an elimination of the larger part of the predominantly low-frequency SGG observation errors. However, the frequency cut-off does allow for the retrieval of low-degree gravity field coefficients, as will be shown below, and an overlap in sensitivity with the SST observations is thus guaranteed. Please note that the design measurement bandwidth for the gradiometer is 5–100 mHz, but a wider spectrum was used to enhance the overlap in sensitivity with the SST observations. The assumed standard deviation (used for weighting the normal equations) for the filtered SGG observations was taken equal to 5 mE, which is comparable with the noise level in the measurement bandwidth.

The two modules described earlier were first used standalone to test their correctness and proper implementation. First, daily precise orbit determinations were conducted, where the kinematic RSO orbit solutions (with 20 s time step) were fitted. Only the orbit parameters and the common-mode accelerometer biases and scale factors (Table 3) were estimated, or 16 parameters per day. A three-dimensional orbit fit of around 25 cm was obtained, reflecting the quality of the prior gravity field modeling and common-mode accelerations. However, this result is based on fixing the common-mode scale factors to 1. It was found that the remaining non-gravitational accelerations are very small due to the DFC leading to large excursions of the estimated scale factors if unconstrained. In fact, this was already shown by simulations, cf. (Visser 2007). Therefore, these scale factors were also fixed to 1 when forming the normal equations for the gravity field estimation, but the observation equations did include the partial derivatives to these scale factors. This will allow the estimation of these scale factors when summing and solving these normal equations (see below). Based on a 30-day test period in June 2010, the common-mode biases (unconstrained estimation) were found to be quite stable, especially for the X direction (Table 4). It has to be noted that in the case of a combined orbit and gravity field parameter determination from both SST and SGG observations, i.e. when the associated normal equations are summed, corrections for the common-mode scale factors are estimated as well. It can thus be stated that for the scale factors of the common-mode accelerometer observations, the implemented method more serves as a validation that the in-flight calibration has been done correctly, i.e. good orbital fits are obtained when the scale factors are taken equal to 1. For example, when not using the common-mode accelerations by taking a scale factor equal to 0, the orbital fit increases typically from 25 to more than 60 cm three-dimensionally, and also much larger values are obtained for the empirical accelerations (increasing from typically below 10 nm/s^2 to more than 70 nm/s^2).

Based on the assumption that the scale factors for all gradiometer SGG observations are already well calibrated by the in-flight procedure and can be kept fixed, the gravitational gradients can be used directly for gravity field retrieval. A 20-day test period was selected covering 28 May to 16 June 2010 and a full 80×80 gravity field recovery was estimated from scratch (i.e. a priori coefficients equal to zero, including J_2) using the three high-pass filtered diagonal gravitational gradient components (decimated to one observation per 20 s). The resulting gravity field is displayed in Fig. 4 in terms of gravity field anomalies: the global match with the pre-launch ITG-Grace2010s model (Mayer-Gürr et al. 2010) is equal to 3.9 mGal compared with a signal magnitude of 20.2 mGal. The dominant part of the gravity field retrieval error is concentrated at the very low degrees. For example, the estimated J_2 coefficient has a relative error of 0.005 (two significant digits) leading to a gravity anomaly error of already more than 2 mGal. Still, it is fascinating that the J_2 coefficient can be derived to this accuracy level from the GOCE SGG observations. In fact, a large part of the gravity field retrieval error displays a rather systematic pattern, which is aligned to a large extent with the orbital ground track (Fig. 4, bottom). This is probably due to remaining systematic (correction) errors outside of the design gradiometer measurement bandwidth (5–100 mHz), e.g. small uncertainties in the exact orientation of the gradiometer reference frame, low-frequency errors in the centrifugal accelerations, etc. Also, it has to be noted that aliasing will occur due to the truncation at degree and order 80. Taking all this into account, the SGG-only solution displayed in Fig. 4 is of remarkably good quality.

Finally, the gravity field and gradiometer calibration parameters were estimated simultaneously by summing the normal equations derived from the kinematic orbit solutions and SGG observations. The 80×80 gravity field coefficients, common mode biases and gradiometer scale factors were fully unconstrained, whereas a Bayesian constraint of 0.01 was applied to the estimation of common-mode scale factors. A total of nine 20-day arcs could be identified in the period staring at 1 November 2009 and ending at 16 June 2010 with a—de facto—uninterrupted stream of GPS SST, star tracker and gradiometer observations. Thus, nine sets of SGG scale factors were estimated and $9 \times 20 = 180$ sets of daily common-mode biases and scale factors.

The mean and RMS-about-mean values of these parameters are included in Table 4. The scale factors for the diagonal SGG observations are within 0.01 from 1. In fact, the associated RMS-about-mean values indicate that the scale factors

Table 4 Estimated calibration parameters

The common-mode biases are represented by CM_i, and the scale factors by SFC_i and SFV_{ii} for the common-mode and gravitational gradient observations, respectively ($i = X, Y, Z$)

Bias (nm/s^2)	CM_X	CM_Y	CM_Z
Module 1 test (June 2010)	-186.7 ± 1.1	314.2 ± 80.5	-658.7 ± 10.5
Selected 20-day periods	-186.7 ± 1.5	291.9 ± 85.5	-77.3 ± 21.2
Scale factors common-mode	SFC_X	SFC_Y	SFC_Z
Selected 20-day periods	1.000 ± 0.005	0.997 ± 0.020	1.000 ± 0.004
Scale factors gradients	SFV_{XX}	SFV_{YY}	SFV_{ZZ}
Selected 20-day periods	1.005 ± 0.007	1.008 ± 0.008	1.008 ± 0.006

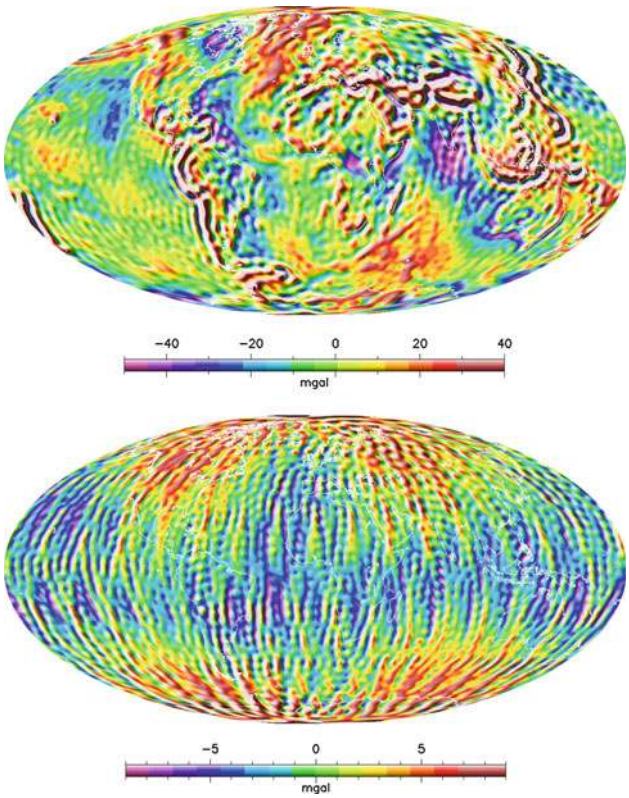

Fig. 4 Gravity anomalies (*top*) from 80×80 gravity field solution from high-pass filtered (fmin = 0.4 mHz) GOCE diagonal SGG observations (data period: 28 May to 16 June 2010) and associated differences with those based on the ITG-Grace2010s model. The RMS of the signal itself (*top*) and the differences (*bottom*) is equal to 20.2 and 3.9 mGal, respectively

are not significantly different from 1. The same might be concluded for the common-mode scale factors. However, possible deviations from 1 for these scale factors were limited by the Bayesian constraints. The formal errors for the common-mode X and Z scale factors were found to be very close to the Bayesian constraint of 0.01, meaning that these factors were hardly determined from the observations. For the common-mode Y factor, the formal error was about 0.008 meaning that this factor was determined by the observations to some extent and still is very close to 1. The common-mode bias could be estimated with a very high consistency level for the X direction and to a lesser extent for the Y and Z directions. The RMS-about-mean values for the common-mode biases are comparable to the formal errors for all three axes, showing the consistency between the results and the estimation process.

2.2.5 *Terrestrial gravity data*

The method of GG calibration with terrestrial data is described in (Bouman et al. 2009) and will here merely be outlined and some results presented. The calibration is based on the gravity data from four regions selected because of available high-quality gravity data and smoothly varying gravity anomalies (Arabelos and Tscherning 1998). The four areas are located in Northern Europe, Canada and Australia, and their geographical distribution is shown in Fig. 5. The area sizes are chosen approximately in the order of $12° \times 12°$. This allows flybys of 200 s duration in each area, which corresponds to the lower part of the MB of 5 mHz.

The calibration method was originally intended to determine GG bias, tilt and SF using LSC (least squares collocation), see (Arabelos and Tscherning 1998; Bouman et al. 2004), which requires the use of a band wise unrestricted GGs and for data distributed over a period of, e.g. 14 days, which would include crossover quality checks and implicit utilization of the Laplace equation. However, as it became clear that the GOCE GGs would be significantly affected by low-frequency noise at a level not compliant to the LSC solution, the approach was changed to handle filtered data. The use of filtered data eliminated the possibility of estimating parameters other than SFs and also eliminated LSC from the direct parameter estimation process.

An alternative method was investigated where GGs are predicted from the terrestrial data with LSC and upward continued to GOCE height. A time series of model GGs are produced and the upward continued GGs replace the model GGs in the calibration areas. This hybrid dataset and the GOCE GGs are band-pass filtered (5–100 mHz) with a sinc filter and for each track crossing the calibration areas SFs for all six GOCE GGs are estimated. Statistics of 750 crossings from the period 19 January to 6 June 2010 are presented

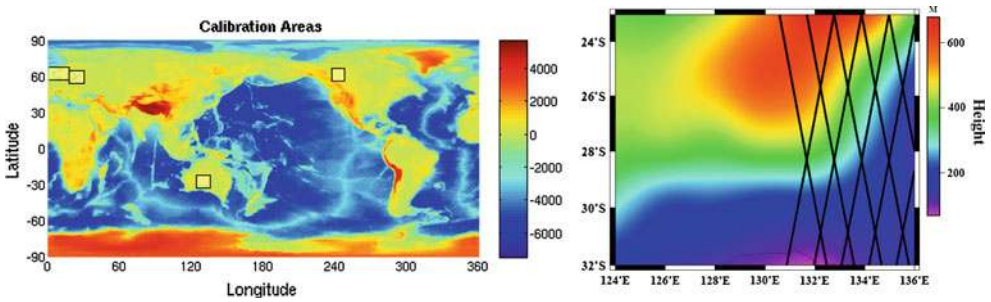

Fig. 5 The calibration areas and the GOCE tracks in the Australian area. Period: 31 October to 13 November 2009

Table 5 Gravitational gradient scale factors statistics in the period January–June 2010

Component	Mean	Median	Standard deviation	Minimum	Maximum
V_{XX}	1.0069	1.0037	0.0570	0.8077	1.2690
V_{YY}	0.9972	0.9966	0.1657	−0.7080	1.8643
V_{ZZ}	1.0063	1.0024	0.0860	0.3178	1.6094
V_{XZ}	1.0037	1.0033	0.0980	0.4343	2.1681

in Table 5. The mean and median values of the SFs are in general close to 1 but the estimates—based on a maximum arc length of only 200 s—are naturally much more volatile compared with, e.g. the GG validation with GPS evaluation period of 20 days, which is also reflected in the sigma values. The large max. and min. values are caused by scale factor estimates affected by Kalman filter reinitialisations. Also for V_{XY} and V_{YZ} scale factors are computed, but these are unreliable because of the larger error on these GGs. Results are not shown.

The calibration with terrestrial data in its present form represents a 'high frequency' GG validation method where larger SF deviations must be expected, but which in general should produce results comparatively close to 1. With the present calibration area size and geographic distribution, approximately three sets of GG SFs are computed each day and can in case of excesses rapidly indicate a malfunction or a calibration issue. The results from the period January to June 2010 shown in Fig. 6 indicate that the SF results seem to be more diffuse at the end of the period (May to June).

In (Bouman et al. 2009) it is discussed in more detail which filtering methods are optimal for the GG filtering, and also the determination of the optimal band pass limits have been discussed frequently regarding the GG calibration. A remarkable result is therefore that SF results calculated for unfiltered GOCE GGs—with only the mean value removed—are equally good or even better than the results for filtered GG. See Fig. 7 in which the SFs for filtered and unfiltered GGs for the period 1 May to 6 June 2010 are shown (only V_{XX} and V_{ZZ} are shown). This indicates that a significant part of the low-frequency noise on the gradients is simply represented as a GG bias for short time intervals.

2.2.6 Gravitational gradient assessment

The GOCE Level 2 gravitational gradients in the GRF (EGG_NOM_2) contain temporal corrections, flags for outliers and the GG scale factors are calibrated/validated using external gravity data. Figure 8 shows a typical example of the Level 2 GGs in the GRF for three orbital revolutions on 1 November 2009. Clearly, the GG signals have a period of 1 CPR. The mean of the GG signals differs significantly from model predictions due to the biases on the measured GGs. Especially the less accurate GGs V_{XY} and V_{YZ} obtain unrealistic values and exhibit larger noise levels as expected.

The errors of the diagonal gravitational gradients have been assessed using a GOCE Quick-Look (QL) gravity field model (Mayerhofer et al. 2010). GGs V_{XX}, V_{YY} and V_{ZZ} from November and December 2009 have been combined with GOCE GPS tracking data to estimate a global gravity field model in terms of spherical harmonic coefficients up to degree and order 200. The GG error assessment is based on an analysis of the GG residuals, i.e. the differences between the measured GGs and those computed with the QL model. Figure 9 displays the spectral densities (SDs) of the estimated GG errors. In the MB the gravitational gradient trace has to fulfil certain requirements that are indicated by the dashed black line. The V_{XX} and V_{YY} errors are approximately flat at a level of around 11 mE/Hz$^{1/2}$ in the upper MB, which is in agreement with the trace requirement. The V_{ZZ} errors are also approximately flat, but the error level is

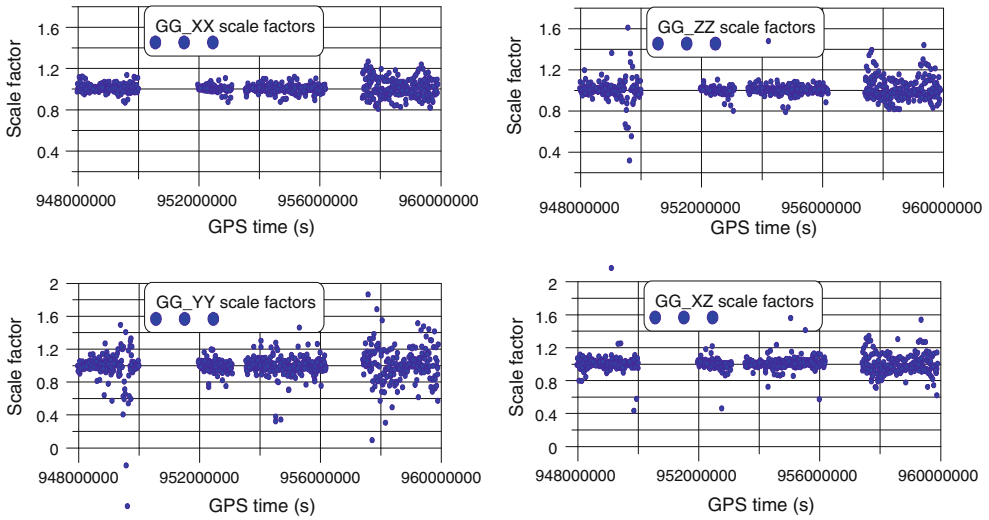

Fig. 6 SF results from period 19 January to 6 June 2010

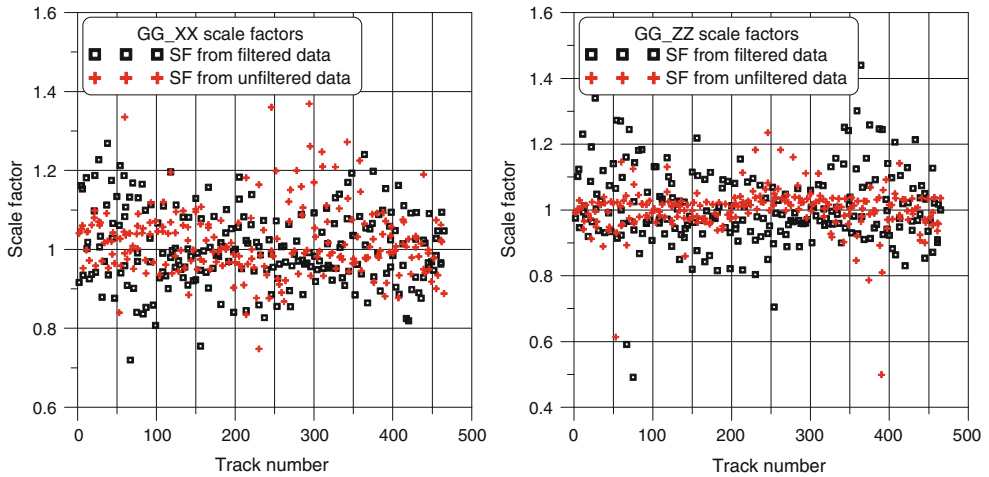

Fig. 7 Comparison of SF determined from filtered and unfiltered data. First track number is from 1 May 2010

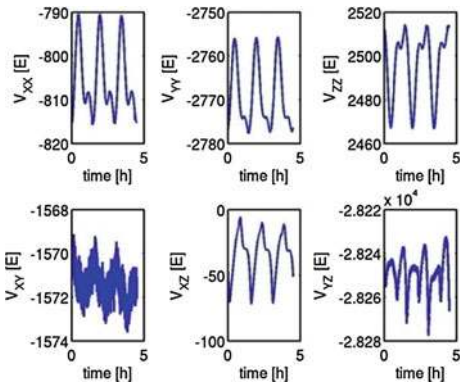

Fig. 8 Gravitational gradients in the GRF (EGG_NOM_2), 3 revolutions 1 November 2009

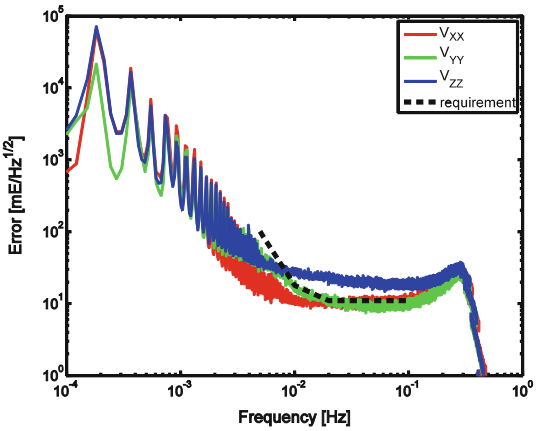

Fig. 9 Estimated GG error SDs

20 mE/Hz$^{1/2}$ or higher. The reason for this higher noise level is not well understood and is under investigation. In the lower MB, between 5 and 10 mHz, the requirement on the GG trace is such that the error is allowed increase to reach 100 mE/Hz$^{1/2}$ at 5 mHz. The errors of all three diagonal gravitational gradients are below this requirement in the

lower MB. Below the MB the errors increase as 1/f, with f the frequency.

3 Rotation of the gravitational tensor

The GOCE Level 2 gravitational gradients are delivered in two versions, with the product names EGG_NOM_2 and EGG_TRF_2. The GGs in the instrument frame, the GRF, were discussed in detail in Sect. 2. The GGs in an Earth-related frame, the LNOF (local north oriented frame), will be discussed here. On the one hand, we will assess the quality of these gravitational gradients and show their information content. On the other hand, we will show and discuss the contribution of the GOCE and model GGs in the LNOF. The X-axis of the LNOF points North, the Y-axis West and the Z-axis in negative radial direction.

3.1 Limitations and solutions

A direct point-wise rotation of the GOCE GG from the GRF to the LNOF, or any other frame, would project the larger GG error of V_{XY} and V_{YZ} onto the other GGs. A method that would not have this disadvantage is a point-wise rotation with the GOCE V_{XY} and V_{YZ} GGs replaced by model GGs, for example computed with a GOCE-only global gravity field model (Pail et al. 2011). Because of the 1/f behaviour of the GG error below the MB, leakage effects may occur. That is, as a result of the frame transformation, long wavelength errors in the GRF may leak to higher frequencies in the LNOF. The signal below the MB for all GGs is therefore also replaced by model signal, for example from a GRACE-based global gravity field model. The idea is to keep as much as possible the GOCE GG signal in the MB, while the signal below the MB is replaced with model GG signal (Bouman 2007; Fuchs and Bouman 2011).

The combination of GOCE GGs in the MB and model GGs below the MB requires that the former are high-pass filtered, whereas the latter are low-pass filtered with the complementary filter. An important parameter that needs to be set is the cut-off frequency of the filter. Fuchs and Bouman (2011) discuss different methods to choose the cut-off frequency. It is based on the estimation of the actual MB, that is, the frequency range in which the GG signal to error ratio is maximal.

Because the GOCE V_{XY} and V_{YZ} GGs in the GRF are replaced by model GGs, the GGs in another reference frame will be a linear combination of GOCE GGs and model GGs also in the MB. For example, if we rotate from the GRF to the LNOF around the Z-axis, the V_{XX} GGs in the LNOF will be a combination of GOCE V_{XX} and V_{YY} GGs in the GRF and model V_{XY} GGs in the GRF. As long as these model GGs in the MB are derived from GOCE-only or GOCE-based gravity field models, this is not necessarily a problem. It is, however, of interest to assess how much the GOCE GGs contribute in the rotated frame and how much the model GGs. This depends on the size of the rotation angle and on the size of the different GG signals (in the MB). We address this issue in the next section.

3.2 Gravitational gradients in the LNOF

In contrast to the GGs in the GRF (Fig. 8), all six GGs in the LNOF have realistic values as Fig. 10 displays. The GGs in the LNOF are shown for a time period of about 4.5 h (three orbital revolutions). The reason is simply that the long wavelength signal comes from a global gravity field model and not from the measured gradients. In addition, the less accurate V_{XY} and V_{YZ} GGs are also determined by a global gravity field model. Note that the qualification 'realistic' does not imply that there are no outliers present in the GGs in the LNOF. Although we tried to detect and flag all outliers a small percentage of small outliers may remain, see Sect. 2.

The diagonal GGs of the rotated gravitational gradient tensor are evaluated using three state-of-the-art global gravity field models, EIGEN-5C, ITG-GRACE2010 and EGM2008 (Förste et al. 2008; Mayer-Gürr et al. 2010; Pavlis et al. 2008). EIGEN-5C and EGM2008 combine GRACE data and tracking data of other satellites with terrestrial gravity data and satellite altimeter data, ITG-GRACE2010 is based on satellite data only. ITG-GRACE2010 is complete to spherical harmonic degree and order $N = 180$, EIGEN-5C to $N = 360$, and EGM2008 has spherical harmonic coefficients up to degree and order $N = 2{,}190$. Model GGs were computed along the GOCE orbit in the LNOF from all three models using the spherical harmonic coefficients up to degree and order $N = 180$ (ITG-GRACE2010) or 360 (EIGEN-5C and EGM2008). The differences of these GGs with respect to the GOCE GGs were computed and these differences were averaged in bins of 0.5° (EIGEN-5C and EGM2008) or 2°

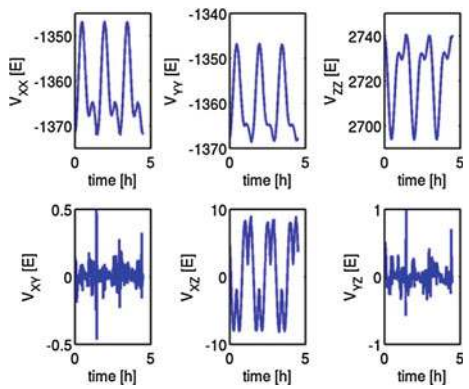

Fig. 10 Gravitational gradients in the LNOF (EGG_TRF_2), 3 orbital revolutions 1 November 2009

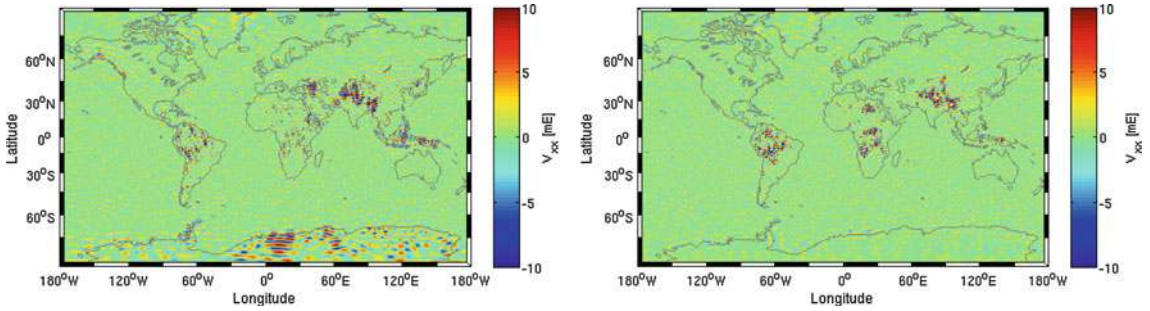

Fig. 11 V_{XX} binned averaged differences 31 October 2009 to 11 January 2010: *Left panel* GOCE–EIGEN-5C ($N = 360$); *Right panel* GOCE–EGM2008 ($N = 360$)

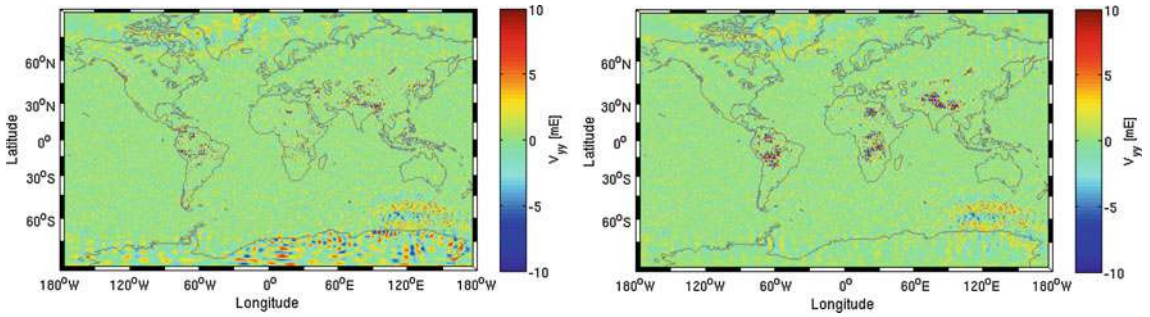

Fig. 12 V_{YY} binned averaged differences 31 October 2009 to 11 January 2010: *Left panel* GOCE–EIGEN-5C ($N = 360$); *Right panel* GOCE–EGM2008 ($N = 360$)

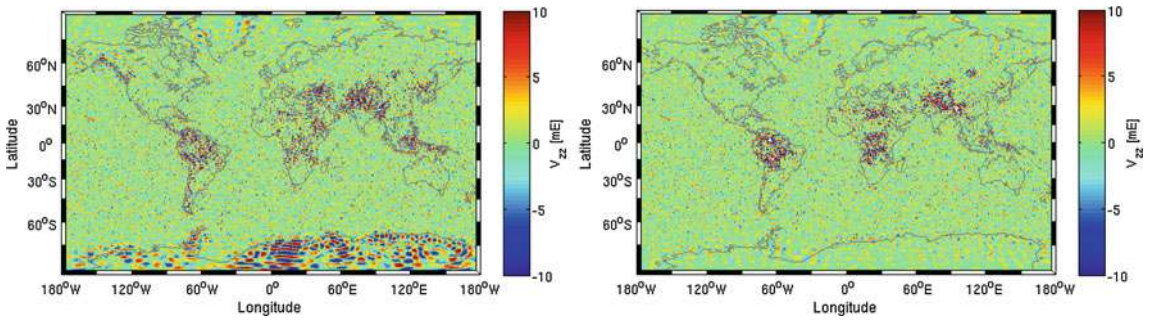

Fig. 13 V_{ZZ} binned averaged differences 31 October 2009 to 11 January 2010: *Left panel* GOCE–EIGEN-5C ($N = 360$); *Right panel* GOCE–EGM2008 ($N = 360$)

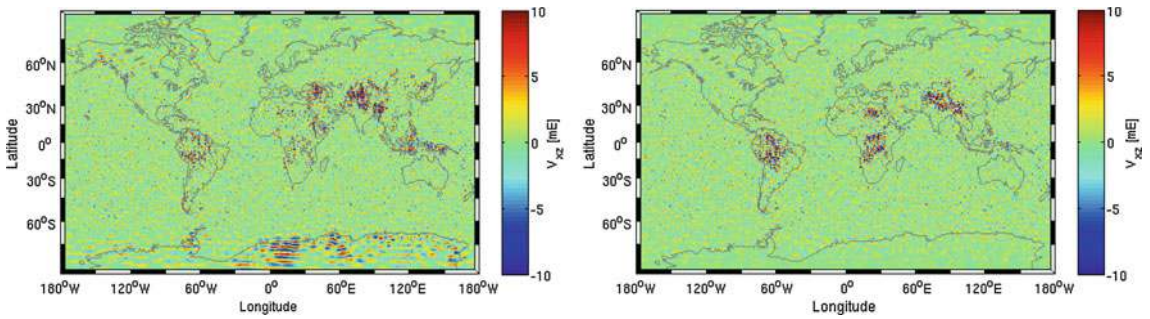

Fig. 14 V_{XZ} binned averaged differences 31 October 2009 to 11 January 2010: *Left panel* GOCE–EIGEN-5C ($N = 360$); *Right panel* GOCE–EGM2008 ($N = 360$)

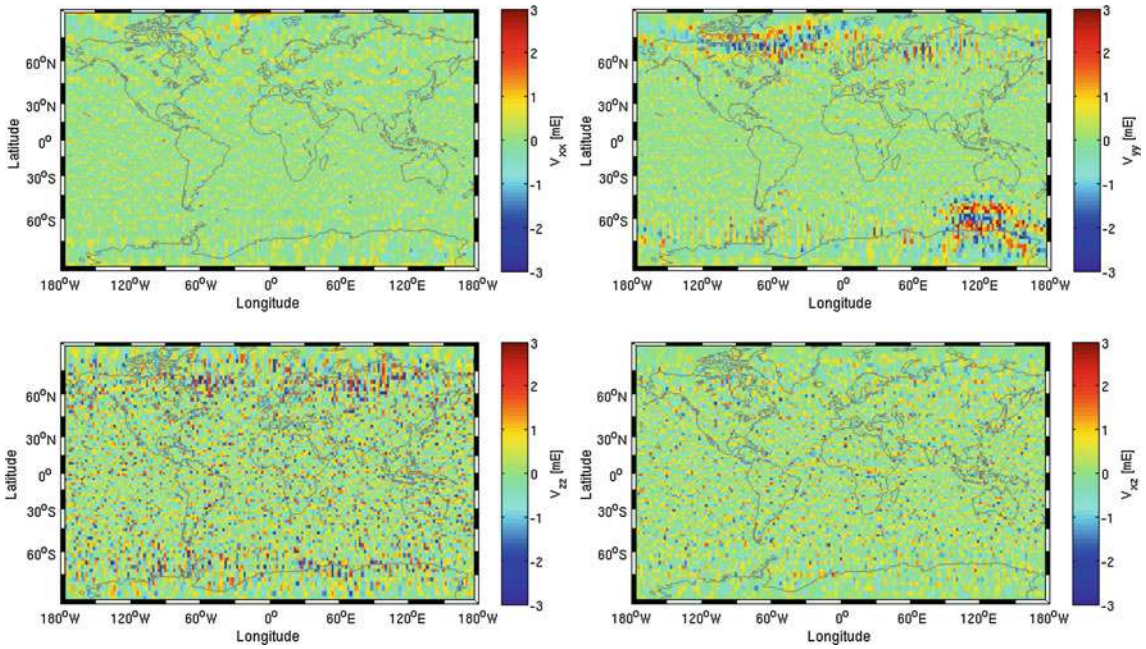

Fig. 15 V_{XX}, V_{YY}, V_{XZ} and V_{ZZ} binned averaged differences 31 October 2009 to 11 January 2010 (*clockwise*): GOCE–ITG-GRACE2010 ($N = 180$)

(ITG-GRACE2010). These binned averaged differences are shown in Figs. 11,12, 13 and 14 for V_{XX}, V_{YY}, V_{ZZ} and V_{XZ} respectively, for EIGEN-5C and EGM2008, and in Fig. 15 for ITG-GRACE2010. The differences were band-pass filtered, which emphasizes the MB where the largest impact of GOCE is expected.

For all three diagonal gravitational gradients the agreement over the oceans between GOCE and EIGEN-5C/EGM 2008 is good. One exception is the region South of Australia and Northern Canada for V_{YY}. These differences do not represent real gravity signal but are probably related to a drift in differential scale factors and can largely be reduced by adjusting the in-flight calibration parameters (Bouman et al. 2010). The agreement between GOCE and EIGEN-5C or EGM2008 over the continents is not so good. Especially in regions where the terrestrial gravity data are known to be of poor quality or not existing, the GOCE and model values are quite distinct. The differences with EIGEN-5C are largest not only in Antarctica, the Himalayas and South-East Asia, but also in Africa and South America. The differences with EGM2008 are the largest in Africa, the Himalaya and South America and to some extent also Antarctica and South–East Asia. Part of these differences may be caused by a sub-optimal weighting of terrestrial gravity data in EGM2008 as discussed in (Förste et al. 2010). In any case, GOCE seems to deliver new valuable gravity field information.

The differences between GOCE and ITG-GRACE2010 are homogeneous in general (note the different colour scales in Fig. 15 compared with Figs. 11, 12, 13, 14). Exceptions are the non-gravitational signatures in V_{YY} close to the magnetic poles as discussed above, as well as the trackiness for high latitudes, especially visible in the V_{YY} and V_{ZZ} differences. The latter are probably caused by the well-known presence of trackiness in GRACE-only solutions, such as ITG-GRACE2010, in North–South direction.

The model content in the GGs in the LNOF is estimated by a separate rotation of GOCE and model gravitational gradients (both sets filtered as described above) and by computing the relative model contribution to the total GG signal confined to the MB (Fuchs and Bouman 2011). The relative model contributions in the LNOF are shown in Table 6 for V_{XX}, V_{YY}, V_{ZZ} and V_{XZ}. The largest rotation from GRF to LNOF is around the Z-axis. Therefore, the relative model content in V_{ZZ} is only 2%. The rotation from GRF to LNOF is large towards the poles where the GRF follows the transition from ascending to descending tracks and vice versa. Thus, the relative model content for the other GGs is largest towards the poles. In addition, the model content in

Table 6 Relative model content in the rotated GGs V_{XX},V_{YY}, V_{XZ} and V_{ZZ}

Gravitational gradient	Model content in LNOF (%)
V_{XX}	25.8
V_{YY}	35.4
V_{ZZ}	1.8
V_{XZ}	21.7

V_{YY} is larger than for V_{XX} because the rotation around roll (X-axis) is larger than the rotation around pitch (Y-axis) and the V_{YY} signal energy in the MB above 12 mHz is smaller compared with V_{XX} (Fuchs and Bouman 2011).

Again it should be noted that the rotated GGs are a combination of GOCE and model values and are therefore biased towards the model that was used. This should be kept in mind when these rotated gravitational gradients are used in, for example, gravity field determination.

4 Conclusions

The GOCE Level 2 gravitational gradients are available in two reference frames: the gradiometer reference frame (GRF) and the local north-oriented frame (LNOF). The GGs in the GRF are derived from the Level 1b GGs by computing and applying temporal corrections, searching and flagging outliers and external calibration of the GGs. The temporal corrections are very small and well below the estimated error level of the gravitational gradients. The percentage of detected outliers is very small, below 0.1% for all GGs. Typical outliers that are not detected are due to slow oscillations in the GG data caused by Kalman reinitialisation after data gaps in the Level 1b processing. Three different external calibration methods have been used to determine GG and/or CM scale factors. Using global gravity field models, we are able to confirm that the GG scale factors do not differ from one down to the 10^{-3} level. This is confirmed by the external calibration with terrestrial gravity and GOCE SST data. The CM scale factors do not seem to differ from one to the 10^{-2} to 10^{-3} level.

Spectral densities of the assessed errors of the diagonal gravitational gradients show that the error of V_{XX} and V_{YY} in the GRF is approximately at the level of the requirement on the gravitational gradient trace in the upper MB, whereas these GG errors are somewhat below the requirement on the trace in the lower MB. The latter is also true for V_{ZZ}, but in the upper MB the error is a factor of 2–3 above the requirement. The exact reason is under investigation. For all three diagonal GGs the error increases as 1/f below the MB.

The GGs in the LNOF are derived from those in the GRF by point-wise tensor rotation. Because the accuracy of V_{XY} and V_{YZ} is much less than that of the other GGs, the less accurate GGs are replaced by model values computed with a GOCE-only gravity field model. Also the GG signal in the GRF below the MB of the accurate GGs is replaced by model signal because of the 1/f error increase. The Z-axes of the GRF and LNOF almost coincide and the model contribution to V_{ZZ} in the LNOF is about 2% on average. For the other accurate GGs the rotations between GRF and LNOF are much larger. Consequently, also the model contribution in the LNOF is larger, up to 35% on average for V_{YY}.

A comparison of the LNOF gravitational gradients with model gravitational gradients from EIGEN-5C and EGM2008, for a period of 10 weeks, shows good consistency over the oceans. Over the continents the consistency can become less, especially in areas with poor terrestrial gravity data. The large differences in these areas with EGM2008 may confirm that the weighting of the terrestrial gravity data in EGM2008 was not optimal. Gravitational gradient differences GOCE–ITG-GRACE2010 are quite homogenous except for trackiness at high latitudes and V_{YY} close to the magnetic poles. The latter is probably related to drift in the gradiometer differential scale factors, whereas the former is probably caused by the well-known trackiness in the GRACE-only gravity field solutions.

Acknowledgments This study was performed in the framework of ESA's project GOCE High-level Processing Facility (No. 18308/04/NL/MM). MF was sponsored by the German Department for Education and Research (Bundesministerium für Bildung und Forschung) as part of the GEOTECHNOLOGIEN program. The NASA Goddard Space Flight Center is acknowledged for kindly providing the GEODYN software. Reinhard Mayrhofer and Roland Pail provided the spectral densities for the errors of the diagonal gravitational gradients. The comments by two anonymous referees helped to improve the paper.

References

Arabelos D, Tscherning CC (1998) Calibration of satellite gradiometer data aided by ground gravity data. J Geod 72:617–625

Bock H, Jäggi A, Meyer U, Visser P, van den IJssel J, van Helleputte T, Heinze M, Hugentobler U (2010) GPS derived orbits for the GOCE satellite. J Geod, GOCE special issue (submitted)

Bouman J (2004) Quick-look outlier detection for GOCE gravity gradients. Newton's Bull 2:78–87

Bouman J (2007) Alternative method for rotation to TRF. GO-TN-HPF-GS-0193, issue 1.0

Bouman J, Koop R (2003) Error assessment of GOCE SGG data using along track interpolation. Adv Geosci 1:27–32

Bouman J, Koop R, Tscherning C, Visser P (2004) Calibration of GOCE SGG data using high–low SST, terrestrial gravity data, and global gravity field models. J Geod 78:124–137

Bouman J, Rispens S, Koop R (2007) GOCE gravity gradients for use in earth sciences. In: Proceedings of the 3rd international GOCE user workshop. ESA-ESRIN, Frascati, Italy, 6–8 November 2006, ESA SP-627

Bouman J, Rispens S, Gruber T, Koop R, Schrama E, Visser P, Tscherning C, Veicherts M (2009) Preprocessing of gravity gradients at the GOCE high-level processing facility. J Geod 83:659–678

Bouman J, Lamarre D, Rispens S, Stummer C (2010) Assessment and improvement of GOCE Level 1b data. J Geod, GOCE special issue (submitted)

ESA (1999) Gravity field and steady-state ocean circulation mission. Reports for mission selection; the four candidate earth explorer core missions. ESA SP-1233(1)

Förste C, Schmidt R, Stubenvoll R, Flechtner F, Meyer U, Koenig R, Neumayer H, Biancale R, Lemoine JM, Bruinsma S, Loyer S, Barthelmes F, Esselborn S (2007) The GeoForschungsZentrum Potsdam/Groupe de Recherche de Géodésie Spatiale satellite-only and combined gravity field models: EIGEN-GL04S1 and EIGEN-GL04C. J Geod. doi:10.1007/s00190-007-0183-8

Förste C, Flechtner F, Schmidt R, Stubenvoll R, Rothacher M, Kusche J, Neumayer H, Biancale R, Lemoine JM, Barthelmes F, Bruinsma S, Koenig R, Meyer U (2008) EIGEN-GL05C—a new global combined high-resolution GRACE-based gravity field model of the GFZ-GRGS cooperation. Geophys Res Abstr 10, EGU2008-A-03426, SRef-ID:1607-7962/gra/EGU2008-A-03426

Förste C, Stubenvoll R, König R, Raimondo JC, Flechtner F, Barthelmes F, Kusche J, Dahle C, Neumayer H, Biancale R, Lemoine JM, Bruinsma S (2010) Evaluation of EGM2008 by comparison with other recent global gravity field models. Newton's Bull 4:18–25

Frommknecht B, Lamarre D, Bigazzi A, Meloni M, Floberghagen R (2011) GOCE level 1b data processing. J Geod, GOCE special issue (submitted)

Fuchs MJ, Bouman J (2011) Rotation of GOCE gravitational gradients to local frames. Geophys J Int (submitted)

Gruber T, Rummel R, Abrikosov O, van Hees R (2007) GOCE level 2 product data handbook. GO-MA-HPF-GS-0110, issue 3.3

Harris FJ (1978) On the use of windows for harmonic analysis with the discrete Fourier transform, In: Proceedings of the IEEE 66, vol 66(1), pp 51–83

IERS (2008) International Earth Rotation Service. http://www.iers.org/. Last accessed 1 july 2008

Koop R, Gruber T, Rummel R (2006) The status of the GOCE high-level processing facility, in 3rd GOCE User Workshop, 6–8 November 2006, Frascati, Italy, pp 199–205, ESA SP-627

Lyard F, Lefevre F, Letellier T (2006) Modelling the global ocean tides: modern insights from FES2004. Ocean Dyn 56(5–6):394–415. doi:10.1007/s10236-006-0086-x

Mayer-Gürr T, Kurtenbach E, Eicker A, ITG-Grace2010 (2010) http://www.igg.uni-bonn.de/apmg/index.php?id=itg-grace2010. Last accessed 15 April 2010

Mayerhofer R, Pail R, Fecher T (2010) Quick-look gravity field solution as part of the GOCE quality assessment. In: Proceedings of the ESA Living Planet Symposium, 28 June–2 July 2010, Bergen, Norway

Migliaccio F, Reguzzoni M, Sansò F (2004) Space-wise approach to satellite gravity determination in the presence of coloured noise. J Geod 78:304–313

Mikhailov V, Pajot G, Diament M, Price A (2007) Tensor deconvolution: a method to locate equivalent sources from full tensor gravity data. Geophysics 72(5):I61–I69

Müller J (2003) GOCE gradients in various reference frames and their accuracies. Adv Geosci 1:33–38

Pail R, Plank G (2004) Gravity field processing strategy. Stud Geophys Geod 48:289–309

Pail R, Bruinsma S, Migliaccio F, Förste C, Goiginger H, Schuh WD, Höck E, Reguzzoni M, Brockmann JM, Abrikosov O, Veicherts M, Fecher T, Mayrhofer R, Krasbutter I, Sansò F, Tscherning CC (2011) First GOCE gravity field models derived by three different approaches. J Geod, GOCE special issue. doi:10.1007/s00190-011-0467-x

Pavlis DE, Poulouse S, McCarthy JJ (2006) GEODYN operations manual, Contract report, SGT Inc., Greenbelt, MD

Pavlis DE, Holmes SA, Kenyon SC, Factor JK (2008) An Earth Gravitational Model to Degree 2160: EGM2008. In: Presented at EGU General Assembly 2008, Vienna, Austria

Pedersen LB, Rasmussen TM (1990) The gradient tensor of potential field anomalies: some implications on data collection and data processing of maps. Geophysics 55(12):1558–1566

Standish EM, Newhall XX, Williams JG, Folkner WF (1995) JPL Planetary and Lunar Ephemerides, DE403/LE403, JPL IOM 314. 10–127

Visser P, van den IJssel J, Koop R, Klees R (2001) Exploring gravity field determination from orbit perturbations of the European Gravity Mission GOCE, J. Geod. 75(2/3):89–98

Visser P (2007) GOCE Gradiometer Validation by GPS, Adv. Space Res. 39(10):1630–1637. doi:10.1016/j.asr.2006.09.014